Received: November 24, 2018

INASS

International Journal of
Intelligent Engineering & Systems

http://www.inass.org/

Segmenting Tooth Components in Dental X-Ray Images Using Gaussian Kernel-Based Conditional Spatial Fuzzy C-Means Clustering Algorithm

Arna Fariza[1,2]* Agus Zainal Arifin[1] Eha Renwi Astuti[3] Takio Kurita[4]

[1]*Department of Informatics, Faculty of Information and Communication Technology, Institut Teknologi Sepuluh Nopember, Indonesia*
[2]*Department of Informatics and Computer Engineering, Politeknik Elektronika Negeri Surabaya, Indonesia*
[3]*Department of Dentomaxillofacial Radiology, Faculty of Dental Medicine, Universitas Airlangga, Indonesia*
[4]*Department of Information Engineering, Graduate School of Engineering, Hiroshima University, Japan*
* Corresponding author's e-mail: arna@pens.ac.id

Abstract: Tooth component segmentation is a crucial task in computer-aided design for forensic odontology, especially to estimate chronological age. Tooth segmentation on radiographic data is a very challenging task due to noise, low contrast, and uneven illumination. The Fuzzy C-Means clustering is generally used for image segmentation that allow pixels to be classified into one or more clusters according to their membership value. However, this clustering method still has problems associated with the shifting of cluster centers and sensitivity to the overlapping intensity distributions between classes. This paper proposes a modified strategy of the conditional spatial Fuzzy C-Means (csFCM) that incorporates global and spatial information into a weighted membership function by replacing the Euclidean distance with the Gaussian kernel distance to increase insensitivity to noise and outliers. The aim of this paper is to divide the tooth into 3 components, i.e. enamel, dentine, and pulp. Therefore, this modified algorithm is preceded by dental X-ray image pre-processing and continued by combining each dental component clusters into one composite image. The tooth image is pre-processed using Contrast Limited Adequate Histogram Equalization (CLAHE) and gamma adjustment to enhance the dental X-ray images quality from the non-uniform lighting. The Gausian kernel-based conditional spatial Fuzzy C-Means (GK-csFCM) segments the dental image into four class clusters, namely enamel, dentine, pulp, and background. Through iterations, the resulting cluster centers are more convergent with real cluster centers, thus ensuring the proposed method improves the drawback of inherent FCM-based methods and further promoting image segmentation performance. The experimental results on the real dental X-ray images showed that GK-csFCM has better performance than the typical FCM and csFCM clustering algorithms in terms of both qualitative and quantitative metrics, i.e. accuracy, specificity, sensitivity, and precision.

Keywords: Tooth component segmentation, Spatial fuzzy c-means, Gaussian kernel based, Dental X-ray.

1. Introduction

Tooth segmentation divides dental X-ray images into isolated parts for different purposes and objectives [1]. This method is widely used by researchers in developing computer-aided design for a variety of real-world problems in the field of dentistry, such as forensic identification of humans, diagnosis of dental disease, dental plaque analysis, age estimation, etc. [2].

Forensic odontologists often use the tooth restoration morphology, for example, enamel, pulp, dentine, etc., for age estimation [3]. Age estimation using panoramic radiography is a non-destructive method that plays an important role in forensic dentistry, which reveals properties that cannot be

seen by physical examination. Age estimation of adults is based on secondary dentine deposition, which occurs without interruption throughout life. Kvall et al. (1995) proposed a method of reducing the pulp area to determine the age of individuals [4]. Using panoramic radiographs, Drusini (2008) identified that a reduction in coronal pulp cavity correlates with chronological age. This is known as the tooth coronal index (TCI) method [5]. The age estimation methods require segmentation of tooth components such as enamel, dentine and pulp which are still done manually. The drawback of manual segmentation is that it is tedious, time-consuming, and user-dependent; for example, it takes hours to segment the maxillomandibular region [6]. Therefore, automated age estimation methods have great potential to increase accuracy and repeatability.

The automatic tooth segmentation based on radiographic data is very challenging due to noise, low contrast, uneven illumination, the complexity of the object topology in the image, random tooth orientation, and the absence of a clear line of demarcation between the tooth and other tissues [7]. Dental X-ray image segmentation falls under machine learning theory, as application of a clustering technique that groups similar values into one group and different values into different groups [8].

Clustering can be done using a hard or a fuzzy approach. Hard clustering is used to divide clusters with well-defined cluster boundaries. However, in real-world applications this method has difficulty because of overlapping cluster boundaries, which causes patterns to be classified incorrectly. Fuzzy clustering improves this by providing more information about the membership of these patterns [9]. A popular fuzzy clustering technique, developed by Bezdek (1981), is Fuzzy C-Means clustering (FCM), which groups patterns based on a fuzzy membership function [10]. In FCM, a pattern's membership of a class cluster is based on certain fuzzy membership degrees [11].

FCM is the most important method for image segmentation by Bezdek et al. (1993). FCM assigns each pixel to a labelled fuzzy cluster and allows pixels to be included in several clusters with various levels of membership [12]. Because of this flexibility, FCM is widely applied in medical image segmentation, because medical images always include unknown uncertainties and noise [13]. Some researchers have further developed the FCM method for medical image segmentation. Huang et al. (2015) proposed a neighbourhood intuitionistic fuzzy c-means clustering algorithm with a genetic algorithm for magnetic resonance imaging (MRI) segmentation [13]. Satheesh and Raj (2017) proposed Multiple Kernel Fuzzy C-Means (MKFCM) clustering techniques for CT scan lung images [14]. Lingappa et al. (2018) developed Kernel Fuzzy C-means (KFCM) clustering to solve noise sensitivity in image segmentation [15]. Gaussian kernel that are induced in objective functions effectively increase insensitivity to noise in the original data space using simpler and more inexpensive [16,17].

Chuang et al. (2006) introduced the spatial FCM (sFCM) algorithm as a variant of FCM that adds spatial information to the FCM membership function [18]. The spatial function considers the value of the neighbouring pixels in the membership function. This spatial function produces a more homogeneous area and eliminates noisy spots and partially reduces spurious blobs. Adhikari et al. (2015) proposed the conditional spatial Fuzzy C-Means (csFCM) clustering algorithm, which incorporates local and global membership in the weighted membership function for magnetic resonance imaging (MRI) [19]. The benefit of the weighted membership function of this algorithm effectively reduces sensitivity to noise and intensity of inhomogeneity. However, this clustering method still has problems associated with the shifting of cluster centers and sensitivity to the overlapping intensity distributions between classes. To overcome this drawback, we propose a modified strategy of the csFCM by replacing the Euclidean distance with the Gaussian kernel distance to increase insensitivity to noise and outliers. The aim of this paper is to divide the tooth into 3 components, i.e. enamel, dentine, and pulp. Therefore, this modified algorithm is preceded by dental X-ray image pre-processing and continued by combining each dental component clusters into one composite image. The tooth image is pre-processed using Contrast Limited Adequate Histogram Equalization (CLAHE) and gamma adjustment to enhance the dental X-ray images quality from the non-uniform lighting. The Gausian kernel-based conditional spatial Fuzzy C-Means (GK-csFCM) segments the dental image into four class clusters, namely enamel, dentine, pulp, and background. Through iterations, the resulting cluster centers are more convergent with real cluster centers, thus ensuring the proposed method improves the drawback of inherent FCM-based methods and further promoting image segmentation performance.

The rest of this paper is organized as follows: Section 2 explains the background of the methodology for tooth component segmentation and related works on this subject. Section 3 explains the methodology of the proposed tooth component segmentation method for dental X-rays. Section 4

presents and discusses the experimental results. Section 5 concludes this paper.

2. Background

In this section, the background of the methodology of multi-class tooth segmentation is briefly reviewed.

2.1 Contrast limited adaptive histogram equalization (CLAHE)

The quality of the digital dental X-rays depends on various factors, such as the sensors, lighting, noise and the captured area [20]. Those factors cause low contrast images that reduces the image quality and inhibit the extracting its useful information process. The denoising filters can reduce noise but degrade the image contrast [20]. Therefore, improving the gray levels of the image in the spatial domain becomes popular methods. The CLAHE is a general contrast enhancement technique that is widely used due to its ease and speed [20-22]. The CLAHE technique and gamma adjustment efficiently increase low contrast in medical imaging, including dental X-rays [22]. CLAHE divides the histogram distribution evenly to increase the contrast of the image. By flattening the gray scale value, the hidden image features to become more visible.

Calculation of the histogram for each region is done directly. In this case, the collection of pixel values for all gray scales is called the histogram of that region. This function is generally obtained by using CDF calculation (Cumulative Distribution Function). If the number of pixels and gray scales in each region, X and Y respectively, and $h_{i,j}(k)$ for k = 0,1,2,. . . , X - 1 is the histogram of region (i,j), then the corresponding CDF calculation, scaled by (X - 1) for gray scale mapping, is:

$$f_{i,j}(k) = \frac{(X-1)}{Y} \cdot \sum_{k=0}^{X-1} h_{i,j}(k) \quad (1)$$

Function (1) is used to change the density function in the gray scale image. This procedure is called histogram equalization. The problem with this method is that the contrast area increases maximally. Limiting the value of the contrast to the desired level is done by limiting the maximum value slope using the β boundary value for the intersection of all histograms. This boundary value (*cliplimit*) can be related to what is called the *clipfactor*, α (in percent), as follows:

$$\beta = \frac{Y}{X}\left\{1 + \frac{\alpha}{100}(s_{max} - 1)\right\} \quad (2)$$

In this case, Eq. (2) is for a *clipfactor* of zero percent, then α = 0 and the value becomes equal to the total image size, which results in pixel value mapping by distributing all region pixels over all gray scales evenly. No change in pixel values will occur. The maximum clip limit, achieved for α = 100, will be changed to the maximum value ($s_{max} = X / Y$). This means that the maximum allowable slope is s_{max}.

2.2 Gamma adjustment

In the context of the explorative contrast enhancement of an image, gamma application is used to set the threshold in image processing [23]. A gamma correction function is used to correct the image's luminance to deal with incorrectly captured luminance. The gamma correction function is used to map the luminance levels to compensate the non-linear luminance effect on display devices. Gamma can be any value between 0 and infinity. If gamma is 1 (the default), the mapping is linear. If gamma is smaller than 1, the mapping is weighted toward higher (brighter) output values. If gamma is greater than 1, the mapping is weighted toward lower (darker) output values.

2.3 Conditional spatial FCM (csFCM)

The FCM algorithm by Bezdek [12] makes it possible to partition n gray value of $X = \{x_1, x_2, ..., x_n\}$ into c cluster by calculating the center of cluster a and membership matrix $U = [\mu_{ij}]$ using objective function $J_m(\mu,a)$, by which m controls the fuzziness of the resulting clustering as follows:

$$J_m(\mu, a) = \sum_{j=1}^{n}\sum_{i=1}^{c} \mu_{ij}^m \left\|x_j - a_i\right\|^2 \quad (3)$$

Objective function usually uses standard Euclidian distance measurement that represents with $\|.\|$. The minimum value is obtained if a high membership value is assigned when the distance of the input pattern is close to the nearest cluster center and a low membership value is assigned if they are far from the cluster center. Fuzzy membership function μ_{ij} and cluster centers a_i are represented in Eqs. (4) and (5):

$$\mu_{ij} = \frac{\|x_j - a_i\|^{-\frac{2}{m-1}}}{\sum_{k=1}^{c}\|x_j - a_k\|^{-\frac{2}{m-1}}} \quad (4)$$

$$a_i = \frac{\sum_{j=1}^{n} \mu_{ij}^m x_j}{\sum_{j=1}^{n} \mu_{ij}^m} \quad (5)$$

Adhikari et al. (2015) developed conditional spatial Fuzzy C-Means (csFCM) that incorporated

spatial and global membership into weighted membership functions [19]. Spatial information considering the interaction between adjacent pixels in the fuzzy membership function helps to reduce the effects of noise and intensity of inhomogeneity in medical images [19]. If adjacent pixels have similar characteristics, then the central pixel will have a higher probability of being in the same group as the adjacent pixels. The spatial information function u_{ij} represents the probability of a pixel being derived from the global membership function as follows:

$$u_{ij} = \frac{h_{ij}\|x_j - a_i\|^{-\frac{2}{m-1}}}{\sum_{k=1}^{c}\|x_j - a_k\|^{-\frac{2}{m-1}}} \quad (6)$$

Spatial function h_{ij} defines the probability of pixel x_j belonging to the i-th cluster by considering its neighborhood in the spatial domain of square window $NB(x_j)$ with M number of neighboring pixels.

$$h_{ij} = \frac{\sum_{k \in NB(x_j)} \mu_{ik}}{M} \quad (7)$$

The csFCM algorithm introduced the weighted membership function z_{ij} and updated cluster center w_i, combining global membership function μ_{ij} and local membership function u_{ij}, assuming they are independent of each other.

$$z_{ij} = \frac{(\mu_{ij})^r (u_{ij})^s}{\sum_{k=1}^{c}(\mu_{kj})^r (u_{kj})^s} \quad (8)$$

$$w_i = \frac{\sum_{j=1}^{m} z_{ij}^m x_j}{\sum_{j=1}^{m} z_{/ij}^m} \quad (9)$$

Parameters r and s control the importance level of both the global and spatial membership functions, respectively.

2.4 Gaussian kernel function

In recent years, machine-learning researchers have widely used kernel methods for pattern recognition and function approximation, for example support vector machine, kernel principal component analysis, kernel perceptron, etc. The aim of adopting a kernel function is inducing a robust distance measure to segment images effectively, inheriting the simplicity of the FCM computation [17].

FCM's kernelization sees every centroid as a data point in the original space and directly transforms it to the feature space and carries out data sample clustering [17]. Let $\Phi(x)$ is the vector x in the feature space F where $\Phi(x) \in F$. If $x=[x_1, x_2]^T$ and $\Phi(x) = \left[x_1^2, \sqrt{2}x_1x_2, x_2^2\right]^T$, where x_i is a component of the vector x. The inner product of $\Phi(x)$ and $\Phi(y)$ in the feature space F is calculated as $\Phi(x)^T\ \Phi(y) = \left[x_1^2, \sqrt{2}x_1x_2, x_2^2\right]^T \left[y_1^2, \sqrt{2}y_1y_2, y_2^2\right] = (x^Ty)^2 = K(x,y)$.

The kernelizing way view every centroid as a data point in the original space like given samples and directly transform them and the data samples into the feature spaces, then modify objective function with the mapping Φ as follows

$$J_m^{\Phi}(\mu, a) = \sum_{i=1}^{c}\sum_{j=1}^{n}\mu_{ij}^m \left\|\Phi(x_j) - \Phi(a_i)\right\|^2 \quad (10)$$

The kernel representation $K(x,y)$ can use to compute the inner products in F without explicitly using transformation Φ. Thus, kernel representation $K(x,a)$ of vector x and a in the d dimension vector is taken as the radial basis function (RBF) and polynomial kernels [17]:

$$K(x, a) = \exp\left(-\frac{\sum_{i=1}^{d}|x_i - a_i|}{\sigma^2}\right) \quad (11)$$

Through the kernel substitution of (10) using inner product, we get

$$\begin{aligned}\left\|\Phi(x_j) - \Phi(a_i)\right\|^2 &= \left(\Phi(x_j) - \Phi(a_i)\right)^T \\ &\quad \left(\Phi(x_j) - \Phi(a_i)\right) \\ &= \Phi(x_j)^T\Phi(x_j) - \Phi(a_i)^T\Phi(x_j) \\ &\quad -\Phi(x_j)^T\Phi(a_i) + \Phi(a_i)^T\Phi(a_i) \\ &= K(x_j, x_j)K(a_i, a_i) - 2K(x_j, a_i)\end{aligned} \quad (12)$$

Furthermore, it is simplified for convenience of manipulation and robustness by using the Gaussian RBF kernel [16,17] as follows:

$$K(x, a) = 1 - K(x_j, a_i) \quad (13)$$

The objective function of FCM using a kernel function is derived from (3) and (10):

$$JS_m^k(\mu, a) = \sum_{i=1}^{c}\sum_{j=1}^{n}\mu_{ij}^m \left(1 - K(x_j, a_i)\right) \quad (14)$$

The equation of $K(x_j,a_i)$ can be simplified as follows [16]:

$$1 - K(x_j, a_i) = 1 - \exp\left(-\frac{\|x_j - a_i\|}{\sigma^2}\right) \quad (15)$$

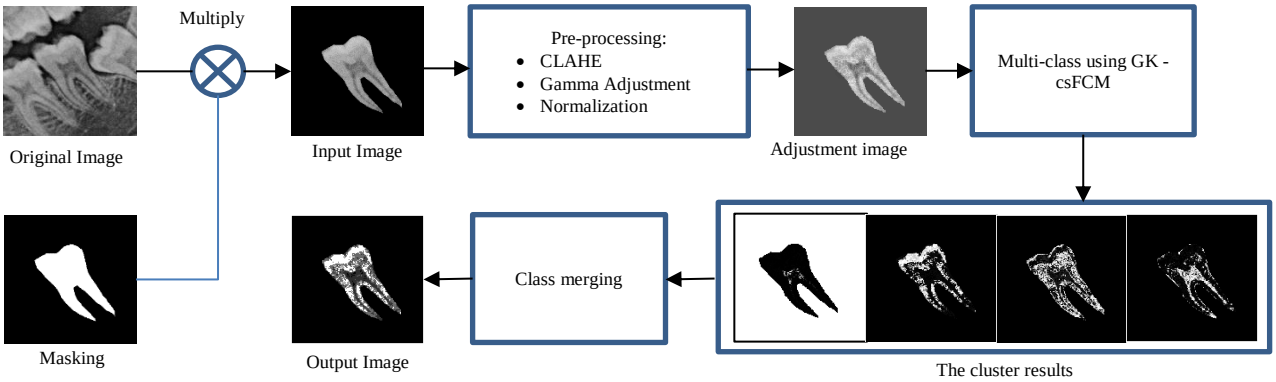

Figure. 1 Steps of the tooth component segmentation process

Notation σ^2 is a variance of the image intensity with mean $\bar{x}$. The variance of each sample input x is represented as:

$$\sigma^2 = \frac{\sum_{i=1}^{d} \|x_i - \bar{x}\|^2}{n} \quad (16)$$

The variance σ^2 is calculated from the global variance pixels and neighborhood variance pixels.

3. Proposed methodology

In this section, we illustrate the steps of tooth component segmentation of dental X-ray images using GK-csFCM. The goal of the framework is segmentation of dental components, consisting of enamel, dentine, and pulp. The steps of the segmentation process are illustrated in Fig. 1.

First, the original image is multiplied by the image mask to get the input image. The input image is pre-processed to enhance the contrast using CLAHE and gamma adjustment and image normalization is also carried out before the segmentation process. The GK-csFCM segmentation produces four clusters, i.e. enamel, dentine, pulp, and background. Then the cluster results are merged to produce the segmented image. The segmented image can be used in automatic age estimation of adults using standard chronological age assessment methods such as Kvall or TCI.

3.1 Input image

The input image was taken from a panoramic radiography image obtained from the Pramita Clinic Laboratory, Sidoarjo, Indonesia. The panoramic radiography image was cropped to leave only the mandible molar areas on the right and left side, as shown in Fig. 2. Image masking was conducted manually in order to separate the area of the tooth, as the region of interest, from the background, gum, tissue, bone and the teeth adjacent to it.

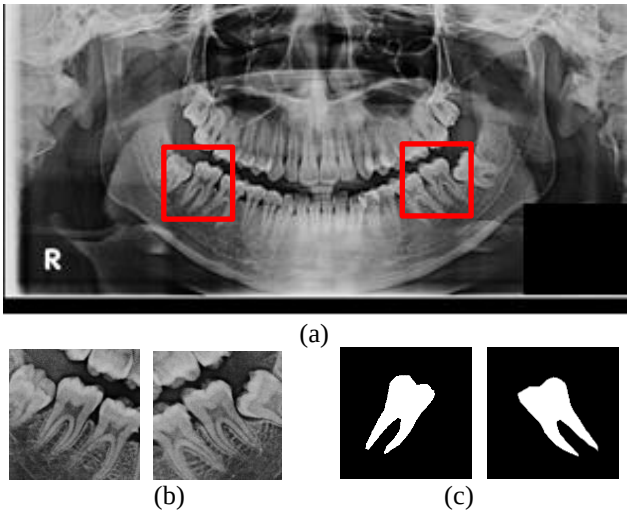

Figure. 2 panoramic radiography image: (a) Panoramic radiography, (b) cropped mandible molar, right and left side, and (c) image masking

The input image came from multiplication of the original image with image masking. The input image is a gray scale image denoted by $X(i,j) \in [0,255]$ with a certain height and weight.

3.2 Image pre-processing

Contrast Limited Adaptive Histogram Equalization (CLAHE) and gamma adjustment are functions that can effectively enhance the gray scale dental images. CLAHE performs contrast-limited adaptive histogram equalization. It operates on small data regions (tiles) rather than the entire image. Each tile's contrast is enhanced so that the histogram of each output region approximately matches the specified histogram (uniform distribution by default).

The contrast enhancement can be limited in order to avoid amplifying noise that may be present in the image. In this paper, the CLAHE method on gray scale dental image X used a 0.002 'ClipLimit' factor to prevent oversaturation of the image, specifically in

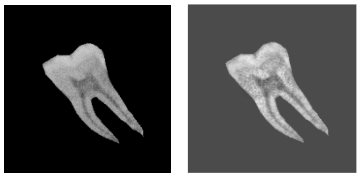

(a) (b)

Figure. 3 Image enhancement result: (a) Input image and (b) image after enhancement

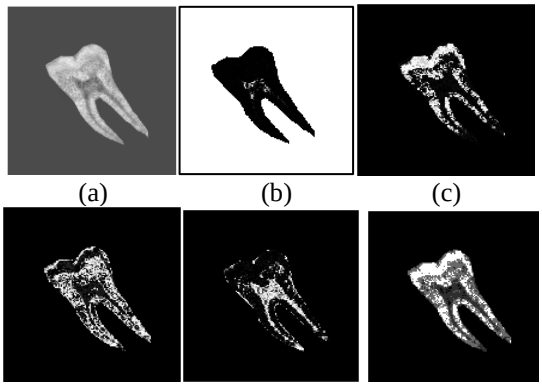

(a) (b) (c)

(d) (e) (f)

Figure. 4 GK-csFCM clustering image: (a) pre-processed image, (b) background cluster, (c) enamel cluster, (d) dentine cluster, (e) pulp cluster, and (f) merged cluster

homogeneous areas and 'rayleigh' distribution to specify the distribution that is used as the basis for creating the contrast transform function.

Gamma adjustment increases the contrast of the image by mapping the values of the input image intensity to new values such that, by default, 1% of the data is saturated at low and high intensities of the input data. To effectively adjust the contrast of a dental gray scale image, a gamma value 0.5 was used (less than 1). The image enhancement result can be seen in Fig. 3. Normalization of the gray scale data into $X(i,j) \in [0,1]$ is useful for the segmentation process.

3.3 Gaussian kernel-based conditional spatial fuzzy c-means (GK-csFCM) clustering algorithm

The pre-processed dental X-ray image was segmented using the Gaussian Kernel-based Conditional Spatial Fuzzy C-Means (GK-csFCM) clustering algorithm and divided into four clusters, respectively representing enamel, dentine, pulp, and background.

The proposed method replaces the Euclidian distance of csFCM with the Gaussian RBF kernel, thus the objective function JS_m^k was modified using Eq. (11). Therefore it derives membership function μ_{ij} and cluster center a_i as follows:

$$\mu_{ij} = \frac{\left(1-K(x_j,a_i)\right)^{-\frac{2}{m-1}}}{\sum_{k=1}^{c}\left(1-K(x_j,a_k)\right)^{-\frac{2}{m-1}}} \tag{17}$$

$$a_i = \frac{\sum_{j=1}^{m}\mu_{ij}^m K(x_j,a_i)x_j}{\sum_{j=1}^{m}\mu_{ij}^m K(x_j,a_i)} \tag{18}$$

This also affects the membership of spatial information function u_{ij}, which represents the probability of the neighboring pixels. The new membership function for the spatial information function is derived from Eq. (6):

$$u_{ij} = \frac{h_{ij}\left(1-K(x_j,a_i)\right)^{-\frac{2}{m-1}}}{\sum_{k=1}^{c}\left(1-K(x_j,a_k)\right)^{-\frac{2}{m-1}}} \tag{19}$$

The use of the Gaussian kernel on the global and spatial membership functions leads to better identification of the similarity between the whole image and the neighboring pixels, making the algorithm more robust for dental X-ray data that are low contrast and inhomogeneity, while handling noise and pixel outliers. The proposed GK-csFCM clustering algorithm consists of the following steps:

Input: Specify the values for number of clusters c, degrees of fuzziness m, r, s, NB, and error ε.

Step 1: Randomly initialize the centers of clusters $a_i^{(0)}$ and the center of joint cluster $w_i^{(0)}$

Step 2: For $t = 1, 2, \ldots, t_{max}$ do

a) calculate membership value $U^{(t)}$ using Eq. (17)
b) calculate conditional spatial membership value $u_{ij}^{(t)}$ using Eq. (19)
c) calculate weighted membership value $z_{ij}^{(t)}$ using Eq. (8)
d) update the center of joint cluster $w_i^{(t)}$ using Eq. (9)
e) update centers $a_i^{(t)}$ using Eq. (18)
f) if $\left\|a_i^t - a_i^{t-1}\right\| < \varepsilon$ then stop

Step 3: Return the center of joint cluster w_i and the weighted membership value z_{ij}; $i = 1, 2, \ldots, c$; $k = 1, 2, \ldots, n$.

The parameters used in this study consisted of the number of clusters $c = 4$, degree of fuzziness $m = 2$, probability level of global membership function $r = 2$ [19], probability level of spatial membership function $s = 2$ [19], spatial window $NB = 3 \times 3$ [19] and error $\varepsilon = 0.001$.

The GK-csFCM clustering algorithm produces 4 clusters from the pre-processed image in Fig. 4 (a) with unsorted cluster values between enamel, dentine, pulp and background clusters, as shown in Fig. 4 (b)-

(d). Each image cluster class produces a graylevel membership value, where white (the highest membership value of gray scale intensity) states the resulting cluster. In the first cluster, Fig. 4 (a) the highest intensity membership value is in the background area. In the second cluster, Fig. 4 (b) the highest intensity membership value is in the enamel area. In the third cluster Fig. 4 (c) the highest intensity membership value is in the dentine area. And in the fourth cluster Fig 4 (d) the highest intensity membership value is in the pulp area.

3.4 Class merging

Tooth component segmentation with the GK-csFCM clustering algorithm is used to obtain the tooth components enamel, dentine, and pulp, which can be used for measurement in an automatic age estimation process. GK-csFCM produces four clustered tooth components, i.e. background (Fig. 4(b)), enamel (Fig. 4(c)), dentine (Fig.4 (d)) and pulp (Fig.4 (e)). The final step is merging the fourth cluster based on the cluster center value, as shown in Fig. 4(f). The merged image indicates each highest intensity of a cluster with a graded color. This aims to distinguish each tooth component by giving them separate gray scale values, i.e. 255 for enamel, 105 for dentine, 46 for pulp, and 0 for the background. The algorithm for merging the 4 clusters into one image is as follows:

1. Prepare Y result image where $Y \in [0,255]$
2. Give index I to each center value of cluster a, with the smallest index as the smallest cluster center value and the largest index as the largest cluster center value.
3. Each cluster index I provides 0, 46, 105 and 255 gray scale a_I =[0,46,105,255] in ascending order.
4. To each pixel $Y(i, j)$ with the z_{ij} membership value in the a_I cluster, which is 1 value, will be given the corresponding gray scale index I value.

4. Result and discussion

This section describes the experimental results on 12 real dental X-rays that had different gray scale contrast intensities. Molar images were selected from panoramic radiography which were seen the boundaries of enamel, dentin and pulp according to the dental forensic standard by the forensic expert. Each image had 258 × 258 pixels and contained the original gray scale image and the masking image. We compared the results of the GK-csFCM clustering algorithm with FCM [12] and csFCM [19]. Note that all images were also pre-processed and after the segmentation process merged in the same way for all

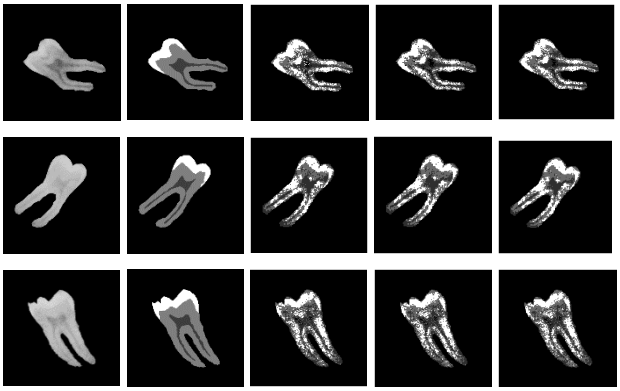

(a) (b) (c) (d) (e)

Figure. 5 Segmentation result of tooth component segmentation using different methods: (a) three input dental X-rays with different contrast, (b) ground truth, (c) segmentation result of the FCM, (d) segmentation result of the csFCM algorithm, and (e) segmentation result of the GK-csFCM algorithm

algorithms. The ground truth images were veryfied and validated by the dental forensic expert.

Fig. 5 shows a comparison of the tooth component segmentation results on the dental X-ray images using FCM, csFCM and the proposed GK-csFCM clustering algorithms. For the comparison, three input dental X-ray images of teeth with different contrasts and ground truths were taken, as shown in Fig. 5 columns (a)-(b). Fig. 5 columns (c)-(d) show the results of segmentation by the FCM algorithm [12] and the csFCM algorithm [19], respectively. Fig. 5 column (e) shows the segmentation result of the GK-csFCM algorithm. As can be seen from Fig. 5, in the segmentation results of the FCM and csFCM algorithms some pixels were grouped together incorrectly, and there is noise in improper areas of the tooth components and in the boundary area between adjacent clusters. Compared to the two methods above, the GK-csFCM algorithm can classify dental components better.

Pre-processing of the data, consisting of CLAHE and gamma adjustment, greatly affects the results of segmentation, as shown by the dental images that have low contrast in the second and third rows. The second row of dental images (Image 10 in Tables 1, 2 and 3) produced an FCM accuracy of 93.3%, a csFCM accuracy of 93.5% and a GK-csFCM accuracy of 93.7%. The third row of dental images (Image 11 in Tables 1, 2 and 3) resulted in an FCM accuracy of 91.2%, a csFCM accuracy of 91.3% and a GK-csFCM accuracy of 91.5%. All of the segmentation results had accuracy greater than 90%.

To analyze the connectivity of the segmented results, details of the tooth parts were extracted to see the segmented tooth components more clearly, as shown in Fig. 6. Fig. 6(a)-(c) show the segmented

dental X-ray images from FCM, csFCM and the proposed GK-csFCM algorithm, respectively. Compared with FCM and csFCM, the proposed GK-csFCM algorithm produced better clusters and reduced the miss-classification, especially in the area around the boundary between the enamel and the background, between the enamel and the dentine area, and also between the pulp and the dentine area.

The performance evaluation of the proposed GK-csFCM segmentation used four clustering metrics, i.e. accuracy, sensitivity, specificity, and precision. These measurements can evaluate the different characteristics of the tooth component segmentation results. Accuracy defines the ratio between the correctly classified enamel, dentine, pulp, not-enamel, not-dentine and not-pulp pixels and the total number of pixels. Sensitivity defines the number of pixels correctly classified as enamel, dentine and pulp divided by the number of enamel, dentine, and pulp pixels of the ground truth. Specificity defines the ratio between the number of pixels correctly classified as background pixels and the number of background pixels of the ground truth. Precision defines the ratio between the pixels correctly classified as enamel, dentine, or pulp and the total number of pixels classified as enamel, dentine, or pulp.

A comparison of accuracy, sensitivity, specificity, and precision of the segmentation of 12 dental X-ray images can be seen in Tables 1, 2, 3 and 4. Tables 1, 2 and 3 respectively show the performance results of the segmentation of the dental X-ray images with the FCM, csFCM and GK-csFCM algorithms. In Tables 1, 2 and 3, it can be seen that GK-csFCM provides high accuracy, sensitivity, specificity, and precision compared to the other, unsupervised algorithms for all input images. Table 4 shows the average matrix of accuracy, sensitivity, specificity and precision, according to which the proposed GK-csFCM algorithm also performed better than the FCM and csFCM algorithms.

The experimental results show that the proposed GK-csFCM algorithm can segment all tooth components accurately, reaching an average accuracy of 93.3%, average sensitivity of 58.1%, average specificity of 95.2% and average precision of 39.6%. These percentages are higher than for FCM and csFCM. The main advantage of the proposed method is that the GK-csFCM algorithm can classify enamel, dentine, and pulp better than the two other algorithms.

The analysis of the segmented results image (qualitative) and performance results of the quantitative metrics, i.e. accuracy, sensitivity, specificity, and precision show the effectiveness of the proposed method GK-csFCM compared with FCM and csFCM for tooth component segmentation such as enamel, dentine and pulp.

(a) (b) (c)

Figure. 6 Tooth areas of the segmented images: (a) segmentation result of FCM algorithm, (b) segmentation result of csFCM algorithm, and (c) segmentation result of GK-csFCM algorithm

Table 1. FCM segmentation performance

No	FCM Performance			
	Accuracy	**Sensitivity**	**Specificity**	**Precision**
1	0.936	0.572	0.955	0.390
2	0.930	0.539	0.950	0.360
3	0.938	0.579	0.956	0.400
4	0.943	0.585	0.960	0.403
5	0.929	0.551	0.949	0.364
6	0.930	0.556	0.950	0.376
7	0.921	0.538	0.943	0.350
8	0.914	0.525	0.938	0.344
9	0.943	0.587	0.959	0.388
10	0.933	0.553	0.952	0.368
11	0.912	0.518	0.937	0.341
12	0.923	0.588	0.944	0.399

Table 2. csFCM segmentation performance

No	csFCM Performance			
	Accuracy	**Sensitivity**	**Specificity**	**Precision**
1	0.936	0.566	0.955	0.386
2	0.932	0.549	0.951	0.369
3	0.939	0.583	0.957	0.402
4	0.944	0.590	0.961	0.408
5	0.929	0.555	0.949	0.368
6	0.929	0.555	0.950	0.375
7	0.920	0.531	0.942	0.344
8	0.913	0.517	0.937	0.338
9	0.945	0.606	0.961	0.406
10	0.935	0.568	0.953	0.382
11	0.912	0.518	0.937	0.341
12	0.921	0.572	0.942	0.384

Table 3. GK-csFCM proposed method segmentation performance

No	GK-csFCM Performance			
	Accuracy	**Sensitivity**	**Specificity**	**Precision**
1	0.940	0.596	0.958	0.413
2	0.933	0.558	0.952	0.377
3	0.943	0.6112	0.960	0.431
4	0.949	0.623	0.964	0.441
5	0.934	0.582	0.952	0.393
6	0.932	0.571	0.951	0.390
7	0.926	0.567	0.946	0.376
8	0.916	0.533	0.939	0.352
9	0.948	0.628	0.963	0.428
10	0.937	0.586	0.955	0.398
11	0.915	0.532	0.939	0.354
12	0.923	0.588	0.944	0.399

Table 4. Average of FCM, csFCM and GK-csFCM segmentation performance

	FCM	**csFCM**	**GK-csFCM**
Accuracy	0.929	0.930	**0.933**
Sensitivity	0.557	0.559	**0.581**
Specificity	0.949	0.950	**0.952**
Precision	0.373	0.375	**0.396**

5. Conclusion

Accurate segmentation of tooth components (enamel, dentine, and pulp) plays an important role in computer-aided design for automatic age estimation. The analysis qualitative show the proposed GK-csFCM algorithm produced better clusters and reduced the miss-classification, especially in the area around the boundary between the enamel and the background, between the enamel and the dentine area, and also between the pulp and the dentine area. The quantitative results showed that the proposed GK-csFCM algorithm segmented enamel, dentine, and pulp better results, i.e. accuracy, sensitivity, specificity, and precision of 39.6% for 12 input images. In the future, the results of this segmentation will be used for an automatic feature extraction that calculates coronal height and the height of the coronal cavity pulp for dental age assessment based on tooth coronal index method [5].

Acknowledgments

The research for this paper was financially supported by the Ministry of Research, Technology and Higher Education, Republic of Indonesia through the Penelitian Disertasi Doktor research scheme. We also thank the Indonesian Endowment Fund for Education (BUDI DN-LPDP), Ministry of Research, Technology and Higher Education, Republic of Indonesia, which fully supported the scholarship.

References

[1] E. Said, G.F. Fahmy, D. Nassar, and H. Ammar, "Dental X-ray Image Segmentation", In: *Proc. of Biometric Technology for Human Identification*, pp.409-418, 2004.

[2] L.H. Son and T.M. Tuan, "Dental Segmentation from X-ray Images Using Semi-Supervised Fuzzy Clustering with Spatial Constraints", *Engineering Applications of Artificial Intelligence*, Vol.59, pp.186–195, 2017.

[3] O.E. Langland, R.P. Langlais, and J.W. Preece, "Principles of Dental Imaging", *Lippincott Williams and Wilkins*, Philadelphia, USA, 2002.

[4] S.I. Kvaal, K.M. Kolltveit, I.O. Thomsen, and T. Solheim, "Age Estimation of Adults from Dental Radiographs", *Forensic science international*, Vol.74, No.3, pp.175–185, 1995.

[5] A.G. Drusini, "The Coronal Pulp Cavity Index: A Forensic Tool for Age Determination in Human Adults", *Cuad Med Forense*, Vol.14, No.53-54, pp.235–249, 2008.

[6] L. Wang, Y. Gao, F. Shi, G. Li, K.C. Chen, Z. Tang, J.J. Xia, and D. Shen, "Automated Segmentation of Dental CBCT Image with Prior-Guided Sequential Random Forests", *Medical physics*, Vol.43, No.1, pp.336–346, 2016.

[7] C.E. Tom and J. Thomas, "Segmentation of Tooth and Pulp from Dental Radiographs", *International Journal of Scientific and Engineering Research*, Vol.6, No.11, pp.115–121, 2015.

[8] M.L. Tangel, C. Fatichah, F. Yan, J.P. Betancourt, M.R. Widyanto, F. Dong, and K. Hirota, "Dental Classification for Periapical Radiograph Based on Multiple Fuzzy Attribute", In: *Proc. of IFSA World Congress and NAFIPS Annual Meeting*, pp.304–309, 2013.

[9] J. Nayak, B. Naik, and H.S. Behera, "Fuzzy C-Means (FCM) Clustering Algorithm: A Decade Review from 2000 to 2014", In*: Proc. of Computational Intelligence in Data Mining - Volume 2*. Springer, pp.133-149, 2015.

[10] J.C. Bezdek, R, Ehrlich, and W. Full, "FCM: The Fuzzy C-means Clustering Algorithm", *Computers and Geosciences*, Vol.10, No.2, pp.191–203, 1984

[11] M.R.P. Ferreiraa and F.A.T. Carvalho, "Kernel Fuzzy C-Means with Automatic Variable

Weighting", *Fuzzy Sets and System*, Vol.237, pp.1–46, 2014.

[12] J.C. Bezdek, L.O. Hall, and L.P. Clarke, "Review of MR Image Segmentation Techniques using Pattern Recognition", *Medical Physics*, Vol.20, No.4, pp.1033–1048, 1993.

[13] C.W. Huang, K.P. Lin, M.C. Wu, K.C. Hung, G.S. Liu, and C.H. Jen, "Intuitionistic Fuzzy C-Means Clustering Algorithm with Neighborhood Attraction in Segmenting Medical Image", *Soft Computing*, Vol.19, No.2, pp.459–470, 2015.

[14] K.G. Satheesh and A.N.J. Raj, "Medical Image Segmentation and Classification Using MKFCM and Hybrid Classifiers", *International Journal of Intelligent Engineering and Systems*, Vol.10, No.6, pp.9–19, 2017.

[15] H.K. Lingappa, H.N. Suresh, and S.K. Manvi, "Medical Image Segmentation Based on Extreme Learning Machine Algorithm in Kernel Fuzzy C-Means Using Artificial Bee Colony Method", *International Journal of Intelligent Engineering and Systems*, Vol.11, No.6, pp.128–136, 2018.

[16] F. Zhao, L. Jiao, and H. Liu, "Kernel Generalized Fuzzy C-Means Clustering with Spatial Information for Image Segmentation", *Digital Signal Processing*, Vol.23, No.1, pp.184-199, 2013

[17] S. Chen and D. Zhang, "Robust Image Segmentation using FCM with Spatial Constraints Based on New Kernel-induced Distance Measure", *IEEE Transactions on Systems, Man, and Cybernetics Part B (Cybernetics)*, Vol.34, No.4, pp.1907–1916, 2004.

[18] K.S. Chuang, H.L. Tzeng, S. Chen, J. Wu, and T.J. Chen, "Fuzzy C-Means Clustering with Spatial Information for Image Segmentation", *Computerized Medical Imaging and Graphics*, Vo.30, No.1, pp.9–15, 2006.

[19] S.K. Adhikari, J.K. Sing, D.K. Basu, and M. Nasipuri, "Conditional Spatial Fuzzy C-Means Clustering Algorithm for Segmentation of MRI Images", *Applied Soft Computing*, Vol.34, pp.758–769, 2015.

[20] H.P. Menon and B. Rajeshwari, "Enhancement of Dental Digital X-Ray Images Based on the Image Quality", In: *Proc. of The International Symposium on Intelligent Systems Technologies and Applications*, Springer, Cham, pp. 33-45, 2016.

[21] Z. Al-Ameen, G. Sulong, A. Rehman, A. Al-Dhelaan, T. Saba, and M. Al-Rodhaan, "An Innovative Technique for Contrast Enhancement of Computed Tomography Iimages Using Normalized Gamma-Corrected Contrast-Limited Adaptive Histogram Equalization", *EURASIP Journal on Advances in Signal Processing*, Vol.32, pp.1-12, 2015.

[22] C.E. Tom and J. Thomas, "Segmentation of Tooth and Pulp from Dental Radiographs", *International Journal of Scientific and Engineering Research*, Vol.6, No.11, pp.115–121, 2015.

[23] A. Karthikeyan, P. Kala, and A. Ramachandran, "Image Quality Improvement in Kidney Stone Detection on Computed Tomography Images", *International Journal of Scientific Research in Science, Engineering and Technology*, Vol.3, No.3, pp.484–488, 2017.